Periodico di Mineralogia (2015), 84, 2, 247-261 DOI: 10.2451/2015PM0012

PERIODICO di MINERALOGIA
established in 1930

An International Journal of
MINERALOGY, CRYSTALLOGRAPHY, GEOCHEMISTRY,
ORE DEPOSITS, PETROLOGY, VOLCANOLOGY
and applied topics on Environment, Archaeometry and Cultural Heritage

AVASPEC 2048: an innovative spectroscopic methodology to differentiate the natural emeralds from the synthetic ones

Alberto Leone[1], Franca Caucia[1,*], Angelo Leone[2] and Luigi Marinoni[1]

[1] Dipartimento di Scienze della Terra e dell'Ambiente, Università di Pavia
[2] Istituto Analisi Gemmologiche, Valenza
[*] Corresponding author: *caucia@crystal.unipv.it*

Abstract

New and sophisticated synthetic gems are constantly introduced in the market making the identification of them very difficult, if one uses only the microscope. In this paper we present the results obtained from a new methodology, the AvaSpec-2048 spectrometer, that can help to identify the natural emeralds from the synthetic ones. The AvaSpec-2048 spectrometer is an original instrument that can acquire electromagnetic spectra in a range between 400 nm and 1000 nm (VIS-NIR), and can be used to identify gemological materials allowing an accurate discrimination of natural products from the artificial ones. The physical and optical properties, microscopic features and absorption spectra of natural and synthetic emeralds have been also investigated through others traditional methodologies such as optical analysis, specific gravities, refractive indices and Vis-NIR spectroscopy. The comparison of the absorption spectra obtained with the AvaSpec-2048 spectrometer could also allow to identify the ore of extraction (and not only the State).

Key words: AvaSpec-2048; spectrometer; emeralds; synthetic emeralds; gemstones.

Introduction

The distinction of natural gemological materials from the synthetic is mostly based on the identification of different peculiar inclusions. Up to now, the only way for distinguishing these gemstones was the observation with microscope, which allows observing the internal features of the cut stones at appropriate magnification (usually 10x to 50x).

Since the early 90's new and sophisticated synthetic gems were constantly being introduced in the market, with physical characteristics and inclusions very similar to those of natural

counterparts. Consequently, the microscope frequently is no longer sufficient to discriminate between the two types of gems, and the identification then become very difficult.

An original instrument that can help for this discrimination is the AvaSpec-2048 spectrometer (Leone, 2012; Leone et al., 2012).

This spectrometer, produced by the Dutch company Avantes, can acquire electromagnetic spectra in a range between 400 nm and 1000 nm (VIS-NIR), and can be used to identify gemological materials allowing an accurate discrimination of natural products from artificial ones (Bernini et al., 2009).

Thanks to its wonderful green color, the emerald has always been considered the most precious variety of beryl and, through the history, it has become one of the most popular gems on the market.

For its beauty and trade value, emerald is one of the most imitated and artificially produced gemstone.

The artificial production of emeralds with a dimension appropriate to be cut as gem was obtained for the first time in the ’30 years in the Farben German laboratories. After the end of the World War II C.F. Chatam obtained emeralds through the method of flux-fusion. The synthetic Chatam gems show a characteristic intense blue-green color, similar to natural samples from Columbia. Specific weight (around 2.65) and refractive indices (1.560 - 1.563) values overlap with natural emeralds from Columbia, Brazil, Zimbabwe and Norway (Leone and Cumo, 1985).

The typical inclusions of the Chatham synthetic products are represented by whitish sheets of flux and veils. Another successful synthetic emerald was the Gilson, which was produced in France. Similarly with Chatam emeralds, the Gilson also show refractive indices (1.563-1.566) and density values that overlap with those of Chatam and natural samples from Columbia, Brazil, Zimbabwe, Norway and, at lesser extent with those from Tanzania, and Russia. The typical inclusions of the Gilson emeralds are represented by prismatic crystals of phenakite, flux particles and biphase levels (Leone and Cumo, 1985).

The production of synthetic emeralds through the hydrothermal process began in the ’60 years in Innsbruck in Austria. Johann Lechleitner produced the first synthetic hydrothermal coating, using some seeds of natural beryl. This product was called *emerita* and shows thin twisted veils, so that the gem appears scratched. These cracks are often filled with liquid drops (healed cracks). Unlike other synthetic emeralds, these gemstones cannot be distinguished from the natural ones solely on their physical parameters. For instance the values of refractive index of these synthetic gems are higher (1.575-1.581) than those of the other synthetic products. Some years later Lechleitner produced synthetic emeralds completely different from the previous ones, they were grown up as a thin layer of green dark emerald on top of a natural colorless beryl lamina, magnified with the deposition of further layers of colorless beryl. Under the microscope these rocks show a banded structure (wafer-like structure; Leone and Cumo, 1985).

Refractive indices and density values of these synthetic gems are very similar to those of natural gems. The typical inclusions are represented by colorless crystals of phenakite, shaped-drape veils and inclusions with form of nail. They have a strong coloration with thickening as a *molasse*, and some inclusions resemble the *trapiche*. A further improvement of the quality of synthetic emeralds was achieved with the emerald Lechleitner III, in which elements like seeds and banded structure are no more observed while nail-shaped inclusions, veils and thin tubular inclusions are still present (Leone and Cumo, 1985).

At the same time, even the U.S. Labs Linde produced hydrothermal synthetic emeralds. These emeralds, obtained from colored seed,

show elongated two-phase inclusions and *swab* crystals of phenakite (Leone and Cumo, 1985).

In the 80's in Perth, Australia, a process of hydrothermal synthesis of emeralds, called Biron, was developed. Also the synthetic emeralds produced with this process showed refractive indices and density values close to those of natural emeralds. The most typical inclusions are represented by oriented fluidizations with triangular shape, altered crystals of phenakite, nails, and hexagonal lines of accretion (Leone and Cumo, 1985).

This paper is aimed to describe and compare the gemological and physical properties of some natural and synthetic emeralds in order to recognize their provenance and the methods of synthesis (molten flux and hydrothermal). All the samples have been investigated through nondestructive methodologies such as the traditional gemological analyses, the microscopic observations and the Avaspec spectroscopy, in order to define parameters that allow characterizing and recognizing the origin of emeralds (Leone and Cumo, 1985).

Material and methods

The emeralds analyzed in this work are 19 natural and 22 synthetic faceted gems (Table 1); they derive from the private collections of the authors, Dr. Angelo Leone, Prof. Franca Caucia and Mr. Carlo Cerutti.

The samples were first examined by standard gemological methods to determine their optical properties, hydrostatic SG and microscopic features. Specific gravity and refractive indices measurements were carried out using a Presidium PCS100 Sensible Balance and a Kruss Rifractometer ER6040 equipment, respectively. Detection limits for refractive indices measurements were $1.30 < n < 1.80$ (Table 2). The gems were examined with a Motic SMZ143 gemological microscope.

Then, the samples were analyzed through the AvaSpec-2048 spectrometer, a CCD (Charge-Coupled Device) based instrument that can acquire electromagnetic waves spectra with wavelengths from 400 to 1000 nm i.e. visible and near infrared. The instrumentation to acquire spectra from gems also include a halogen light source, an integrating sphere placed above a sample holder and fiber-optic conductors cables. All the studied samples were not cooled before being subjected to the light beam and the measurements, therefore, were conducted at room temperature. The instrument does not require cooling of the samples.

AvaSpec is a new non-destructive method, which had never been previously employed to distinguish the gem-quality minerals.

Gemological properties

The appearance and gemological properties of the investigated emeralds are reported in Table 1 and 2. Values of specific gravity of natural samples 1-19 are between 2.65 to 2.81 g/cm^3 while refractive indices are between 1.571 to 1.598, comparable with the range in literature (Leone, 1993; Boiocchi et al., 2004).

Synthetic samples 1 - 22 show values of specific gravity between 2.53 to 2.88 g/cm^3 and values of refractive indices between 1.560 to 1.580.

Microscopic features

The sample 1N from Colombia shows the typical inclusion of the emeralds from this country, i.e., three-phase inclusions formed by brine, vapor and halite (Photo 1). Most of inclusions in Colombian emeralds are liquid and often described as mossy-like or garden-like (Leone, 1993). The sample n. 18N from Muzo mines is the variety called *trapiche* or *gemelos* and exhibits a star pattern formed by a six green radial crystals cemented by dark carbon impurities (Photo 2).

The African emeralds studied in this work

Table 1. Gemological properties of studied samples.

Natural samples	Provenience	Cut	Synthetic samples	Typoligies of synthesis	Cut
1N	Colombia oil treated	oval	1S	flux fusion - Gilson	emerald cut
2N	Colombia oil treated	shield	2S	flux fusion - Gilson	emerald cut
3N	Zambia	emerald cut	3S	flux fusion - Gilson	emerald cut
4N	Zambia	emerald cut	4S	flux fusion - Gilson	emerald cut
5N	Russia	emerald cut	5S	flux fusion - Gilson	emerald cut
6N	Russia	emerald cut	6S	flux fusion - Gilson	emerald cut
7N	Russia	emerald cut	7S	hydrothermal - Lechleitner (emerita) I	emerald cut
8N	Brazil	oval	8S	hydrothermal - Lechleitner II	emerald cut
9N	Brazil	round	9S	hydrothermal - Lechleitner III	emerald cut
10N	Brazil	round	10S	hydrothermal - Lechleitner II	emerald cut
11N	Brazil	round	11S	flux fusion - Chatham	emerald cut
12N	Brazil	emerald cut	12S	hydrothermal - Linde	emerald cut
13N	Brazil	round	13S	hydrothermal - Linde	emerald cut
14N	Brazil	round	14S	hydrothermal- Linde	emerald cut
15N	Brazil	round	15S	hydrothermal - Lechleitner II	emerald cut
16N	Brazil	oval	16S	hydrothermal - Biron	pear
17N	Colombia trapiche	oval	17S	hydrothermal - Biron	octagon
18N	Colombia trapiche	oval	18S	hydrothermal - Biron	oval
19N	Colombia	emerald cut	19S	hydrothermal - Biron	oval
20N	Colombia oil treated	rough	20S	flux fusion - Chatham	rough
21N	Colombia oil treated	oval			

come from Zambia (sample n. 3N and n. 4N). Under the microscope they show orientated negative crystals (Photo 3); irregular black dendrites of ilmenite are also frequently present (Photo 4).

Russian emeralds (sample n. 5N) present two-phase inclusions frequently randomly arranged (Photo 5). In the sample n. 6N we observe

Table 2. Gemological properties of studied samples.

Natural samples	weight (ct)	specific gravity	refractive indices (nε - nω)	Synthetic samples	weight (ct)	specific gravity	refractive indices (nε - nω)
1N	4.59	2.70	1.571 - 1.579	1S	1.13	2.56	1.560 - 1.565
2N	3.89	2.73	1.580 - 1.586	2S	0.98	2.64	1.561 - 1.566
3N	0.93	2.74	1.587 - 1.591	3S	0.91	2.53	1.560 - 1.565
4N	0.51	2.74	1.587 - 1.593	4S	0.65	2.60	1.560 - 1.565
5N	0.89	2.77	1.582 - 1.590	5S	0.81	2.66	1.560 - 1.565
6N	0.73	2.70	1.582 - 1.590	6S	0.87	2.66	1.560 - 1.565
7N	0.67	2.72	1.578 - 1.583	7S	1.99	2.72	1.579 - 1.586
8N	1.39	2.71	1.588 - 1.592	8S	0.75	2.59	1.575 - 1.580
9N	0.19	2.71	1.585 - 1.590	9S	0.60	2.66	1.560 - 1.563
10N	0.30	2.69	1.587 - 1.591	10S	1.50	2.63	1.572 - 1.580
11N	0.50	2.70	1.587 - 1.592	11S	2.26	2.66	1.560 - 1.566
12N	1.01	2.68	1.589 - 1.593	12S	0.65	2.64	1.575 - 1.579
13N	0.34	2.69	1.588 - 1.592	13S	0.93	2.66	1.560 - 1.568
14N	0.30	2.69	1.588 - 1.592	14S	0.65	2.66	1.560 - 1.565
15N	0.50	2.71	1.588 - 1.594	15S	0.47	2.68	1.570 - 1.575
16N	1.63	2.81	1.590 - 1.598	16S	0.99	2.67	1.570 - 1.578
17N	0.84	2.71	1.578 - 1.582	17S	1.57	2.67	1.570 - 1.575
18N	0.69	2.65	1.578 - 1.584	18S	0.20	2.88	1.570 - 1.578
19N	0.82	2.73	1.575 - 1.580	19S	0.54	2.68	1.572 - 1.580
20N	7.23	2.74	1.570 - 1.578	20S	0.22	2.75	1.560 - 1.570
21N	5.53	2.67	1.573 - 1.580				

other textures typical of Russian emeralds: thin planes, parallel to each other, formed by smaller gas bubbles that appear brightly iridescent when enlightened with interfering light (Photo 6).

The samples n. 8N and n. 16N, from Brazil, appear rather blurred; the sample n. 8N under the microscope exhibits black points and brownish laminate inclusions that are made up by crystals

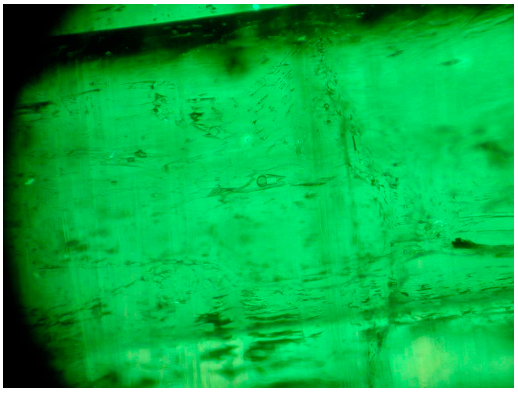

Photo 1. Colombian emerald (sample n. 1N), three-phase inclusions.

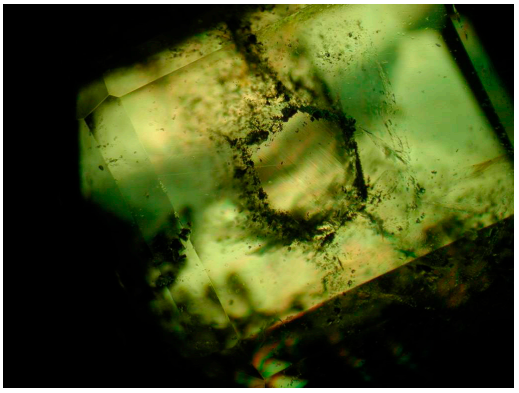

Photo 2. Colombian emerald from Muzo mines (sample n. 18N), trapiche

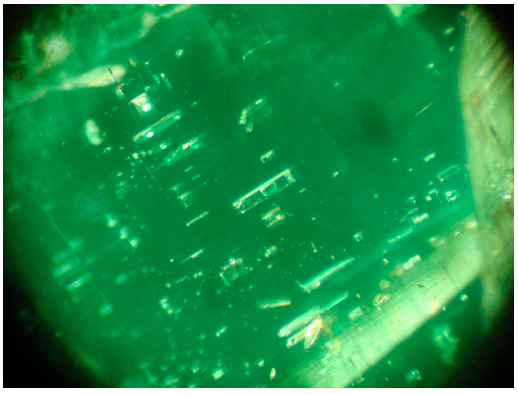

Photo 3. African emerald (sample n. 3N), negative crystals.

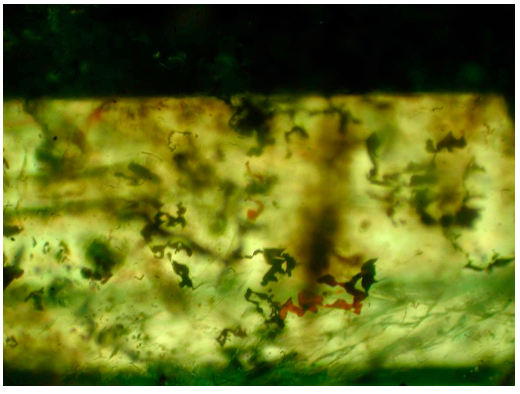

Photo 4. African emerald (sample n. 4N), irregular black dendrites of ilmenite.

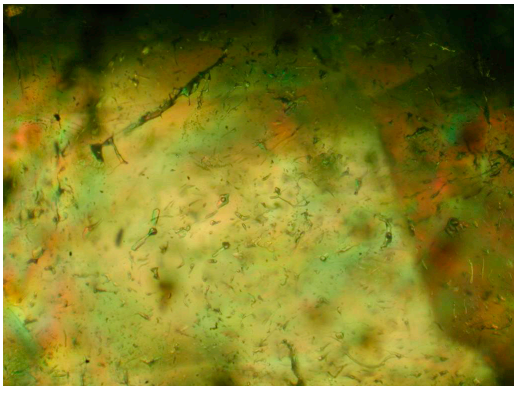

Photo 5. Russian emerald (sample n. 5N), two-phase inclusions arranged disorderly.

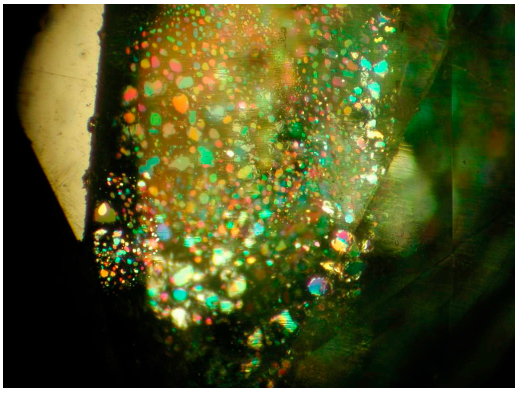

Photo 6. Russian emerald (sample n. 6N), interference colors due to gas bubbles.

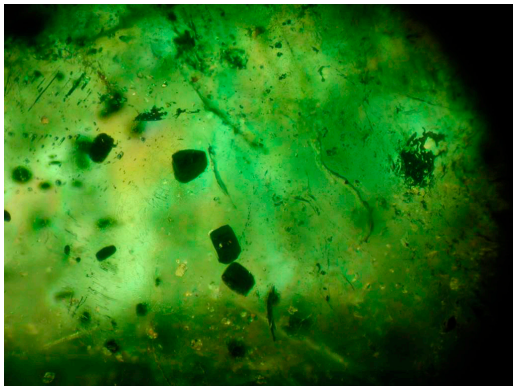

Photo 7. Brazilian emerald (sample n. 8N), magnetite black crystals and brownish laminates of biotite-flogopite.

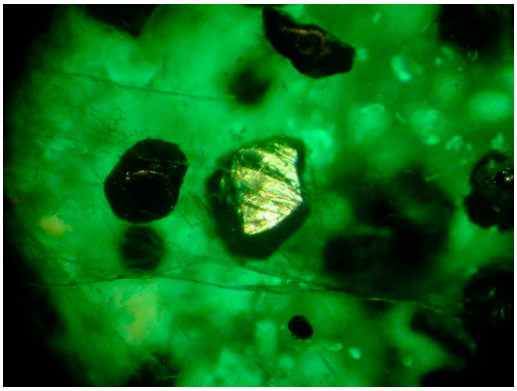

Photo 8. Brazilian emerald (sample n. 16N), pyrite crystals.

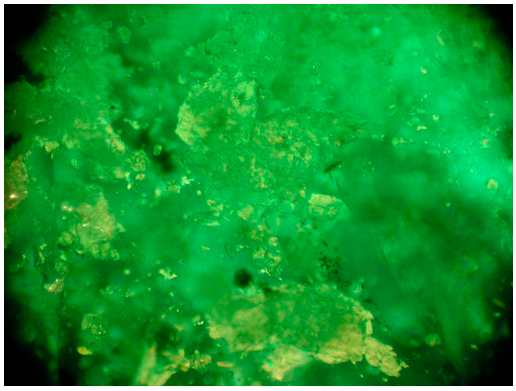

Photo 9. Brazilian emerald (sample n. 12N), aggregate of calcite crystals.

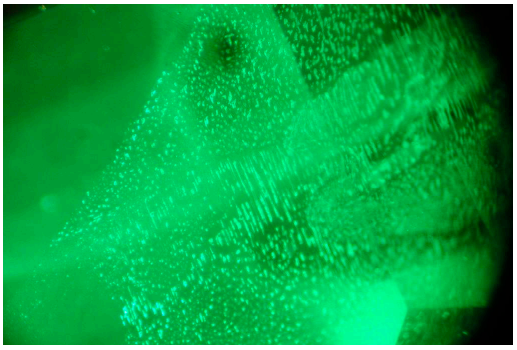

Photo 10. Gilson synthetic emerald (sample n. 1S), liquid veils.

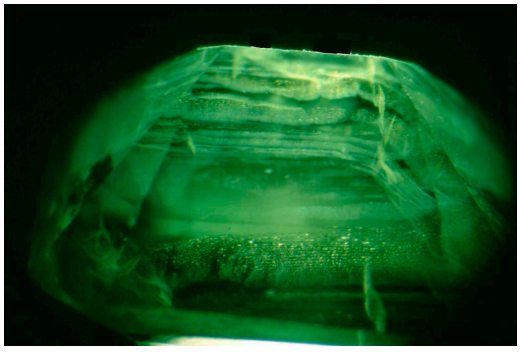

Photo 11. Gilson synthetic emerald (sample n. 4S), flux residue and phenakite crystals.

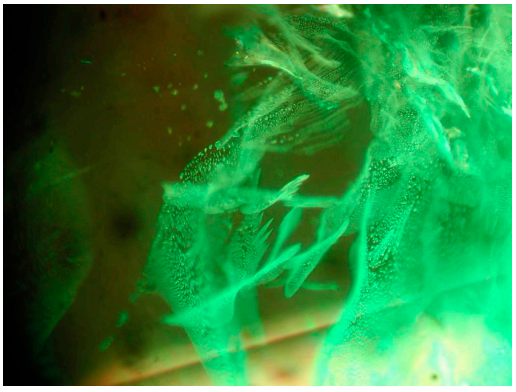

Photo 12. Chatam synthetic emerald (sample n. 20S), tangled veils and flux residue.

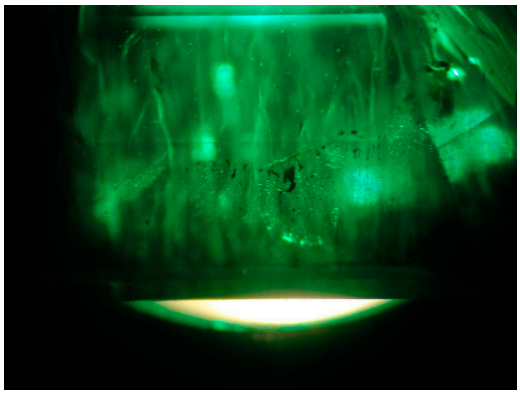

Photo 13. Biron synthetic emerald (sample n. 16S), fluidizations and veils.

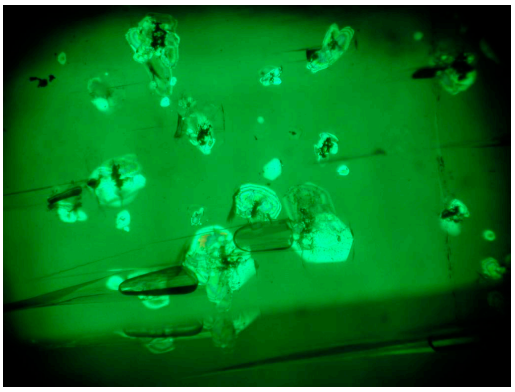

Photo 14. Biron synthetic emerald (sample n. 17S), nail-head inclusions.

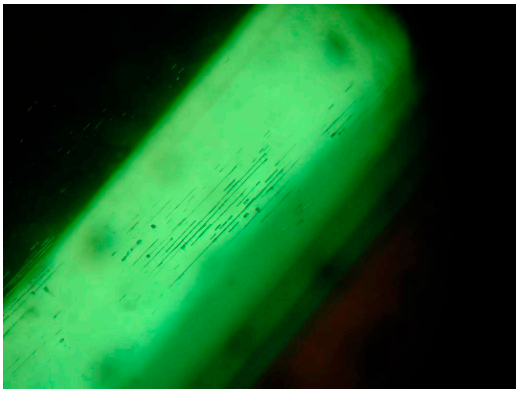

Photo 15. Linde synthetic emerald (sample n. 13S), two-phase inclusions.

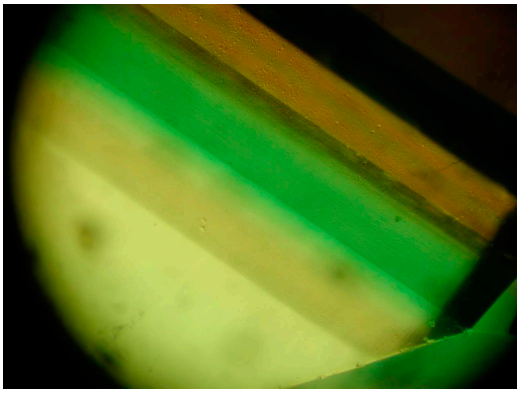

Photo 16. Linde synthetic emerald (sample n. 14S), parallel growing lines.

Photo17. Emerita synthetic emerald (sample n. 7S), grid-like veils on the surface.

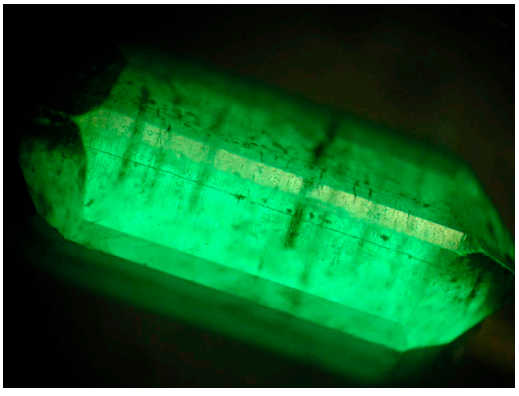

Photo 18. Lechleitner II synthetic emerald (sample n. 8S), colorless seed and growing lines.

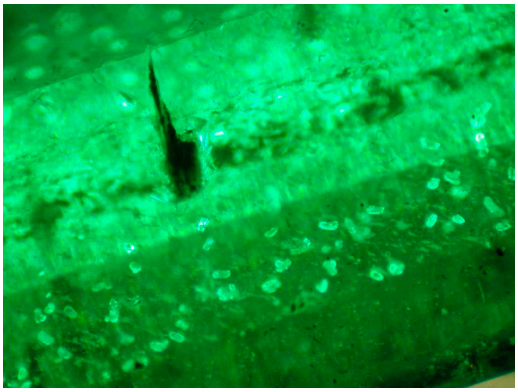

Photo 19. Lechleitner II synthetic emerald (sample n. 15S), blackish phenakite crystals.

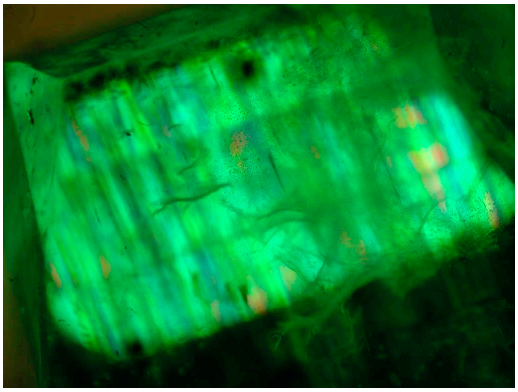

Photo 20. Lechleitner III synthetic emerald (sample n. 9S), "nail-head" inclusions and tangled veils.

of magnetite and biotite-flogopite (Photo 7). In sample n. 16N we can observe a crystal of pyrite (Photo 8) while in sample n. 12N we observe some calcite crystals that, in some cases, appear as an aggregate (Photo 9).

In the synthetic Gilson samples (molten flux) the most frequent inclusions are liquid veils, like in sample n. 1S (Photo 10). In the sample n. 4S other small and translucid inclusions due to the flux residue, as well as phenakite crystals, are found (Photo 11).

The sample n. 20S (Chatam synthetic emerald) shows tangled veils that compromise the transparency (Photo 12). Moreover, the same sample displays some white opaque flux residue.

The typical inclusions of the Biron synthetic emeralds (hydrothermal) are the fluidizations parallel to the c axis of the crystal with the triangular growth section visible in the sample n. 16S. In the same sample there are also veils formed by liquid inclusions (Photo 13). The sample n. 17S shows the nail-head spicules: a two-phase (liquid and gas) inclusions capped with a phenakite crystal (Photo 14).

The Linde synthetic emeralds (hydrothermal) exhibit thin veils formed by two-phase inclusions, like in the sample n. 13S (Photo 15). The sample n. 14S shows the green seed where the growth begins with the parallel growing lines (Photo 16).

Sample n. 7S is an *Emerita* synthetic emerald (hydrothermal) also known as Lechleitner I; is generally colorless, covered with a thin layer (about half a millimeter) of synthetic emerald that is recognizable at the microscope because of a grid-like veils extended all over the surface of the gemstone (Photo 17).

The samples n. 8S and n. 15S are Lechleitner II synthetic emeralds (hydrothermal): the colorless seed is clearly observable in contrast light under the microscope (Photo 18). Cloudy inclusions due to blackish pile of colorless phenakite crystals (nail-head) are visible in sample n. 15S (Photo 19).

The synthetic emerald n. 9S is a Lechleitner III (hydrothermal and development of the Lechleitner II) with higher clearness. Nail-head inclusions are still evident but not the growth seed; instead, it is possible to observe tangled veils (Photo 20).

Avaspec-2048 Data

All analyzed samples were faceted and not oriented in a crystallographic direction. For this reason, many absorption bands and peaks may

not be visible or may be slightly shifted in the absorption spectra.

The absorption spectra of the analyzed emeralds have been divided in three main groups: i) natural, ii) synthetic obtained by hydrothermal techniques and iii) synthetic obtained by molten flux.

Green beryl (emerald) is colored by the Cr^{3+} ions occurring in the octahedral Al^{3+} sites and, whether the emeralds were natural or synthetic, the chromium spectrum shows two broad bands near 430 and 600 nm and three absorption peaks at 476, 680 and 683 nm (Wood et al., 1968; Anderson, 1987; Fenoll et al., 2007; Flamini et al., 1984).

Pale green beryls and emeralds are also colored by iron ions that produce some typical spectral lines: a strong band at 810 nm and an absorption band at 465 nm in the ultraviolet region. The latter line is due to the crystal field 3d-3d transitions in the ferric ion and this Fe^{3+} line does not contribute to the color of the crystal (Wood et al., 1968). The absorption spectra of all analyzed samples are described below.

Absorption spectra of natural emeralds

Absorption spectra between 400 nm and 700 nm are very similar in all the investigated natural emeralds showing absorption bands and peaks related to Cr^{3+} and $Fe^{3+/2+}$ (Flamini et al., 1983).

- *Natural samples from Colombia (Figure 1).* The Colombian samples show two broad absorption bands at 450 and 600 nm and a peak at 665 nm, that is related to Cr^{3+} (Wood et al., 1968). We also observe absorption peaks at 410, 423 and 450nm, that can be attributed to Fe^3 ions (Wood et al., 1968).
- *Natural oil-treated samples from Colombia (Figure 2).* These samples show a broad band at 450 nm and a wide plateau between 520 and 700nm (less evident in the sample n. 1N). The absorption band at 450 nm and the absorption peaks at 590 and 610 nm are related to Cr^{3+} (the last peak is evident only in the spectrum of sample n. 1N; Wood et al., 1968). The plateau was observed only in the emeralds filled with oil. We also observe absorption peaks at 410, 423 and 450, that are due to Fe^{3+} (Wood et al., 1968).
  In all the samples the absorption peak at 955 nm, related to H_2O, is clearly evident (Wood et al., 1968).
- *Natural samples from Zambia (Figure 3).* The samples from Zambia show three absorption peaks at 420, 450 and 470-480 nm and another at 680 nm, all related to Cr^{3+} (Wood et al., 1968). The broad absorption band at 600nm is much less intense then that of Columbian emeralds: this could be due to high content of vanadium in the samples from Zambia. If this hypothesis were confirmed, it could represent an additional parameter of identification. We also observe a negative peak at about 800 nm that can be attributed to Fe^{2+} (Wood et al., 1968) that was not present in the other samples.
- *Natural samples from Russia (Figure 4).* At low wavelengths the spectra of these samples show a ground noise higher than that of the other natural emeralds. The spectra of Russian emeralds show three main absorption bands between 400 and 500 nm, at 415, 440 and 475 nm that are due to the presence of Cr^{3+} (Wood et al., 1968). The peak at 680 nm is too weak to be considered a discriminating feature of the spectrum. We also observe a wide band centered at 830 nm and a peak at about 950 nm due to the presence of H_2O (Wood et al., 1968; Adamo et al., 2005). The absorption peaks at 405 and 465 nm are related to Fe^{3+} ion (Wood et al., 1968).
- *Natural samples from Brazil (Figure 5).* These samples show a broad absorption band at 450-460 nm due to Fe^{3+} and a broad

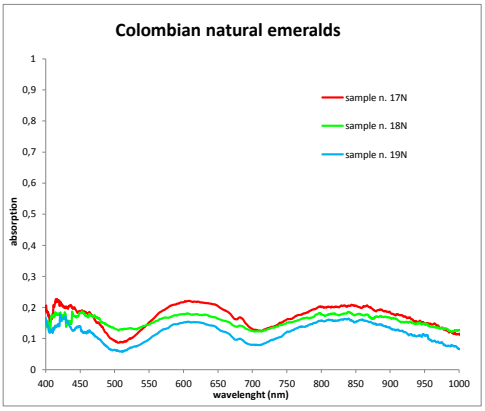

Figure 1. AvaSpec-2048 absorption spectra of Colombian natural emerald n. 17N, 18N, 19N.

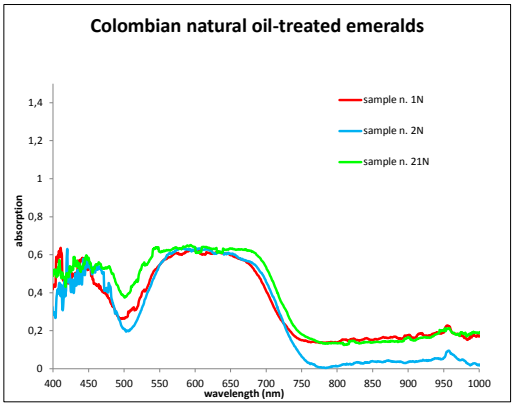

Figure 2. AvaSpec-2048 absorption spectra of Colombian natural oil-treated emerald n. 1N, 2N, 21N.

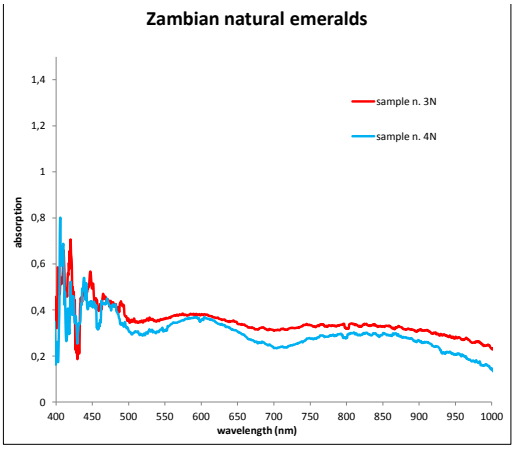

Figure 3. AvaSpec-2048 absorption spectra of Zambian natural emerald n. 3N, 4N.

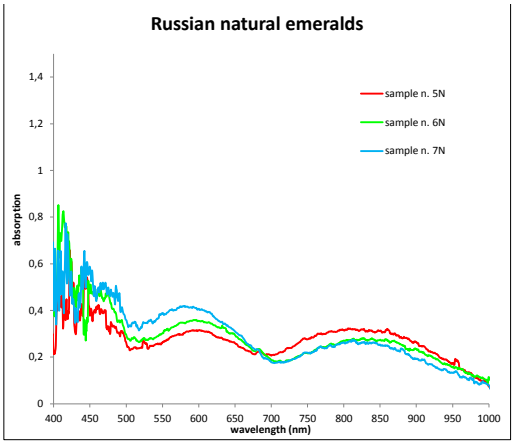

Figure 4. AvaSpec-2048 absorption spectra of Russian natural emerald n. 5N, 6N, 7N.

band at 600 nm related to Cr^{3+} (Wood et al., 1968).

The absorption band related to Fe^{3+} at low wavelengths is more evident in these samples than in the other natural ones; this can be attributed to the yellowish shade that characterizes the Brazilian emeralds.

Absorption spectra of synthetic emeralds

Flux fusion synthesis

- Chatam synthetic sample (Figure 6).
  In this sample we observe a broad absorption band at about 600 nm, a broad band between 450 and 500 nm and a peak at 415 nm that are related to Cr^{3+} (Wood et al., 1968). The

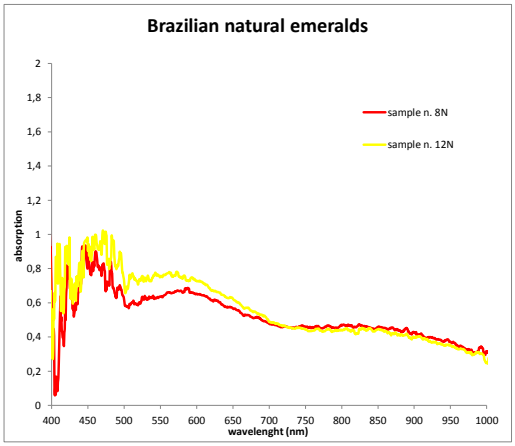

Figure 5. AvaSpec-2048 absorption spectra of Brazilian natural emerald n. 8N, 12N.

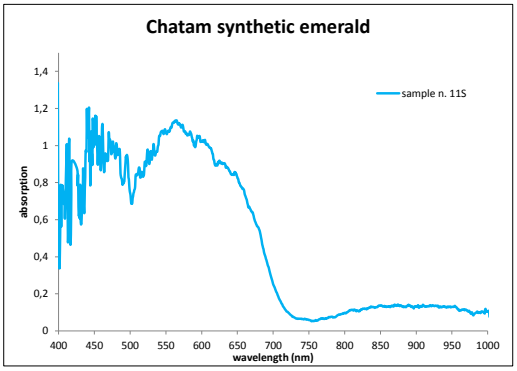

Figure 6. AvaSpec-2048 absorption spectra of Chatam synthetic emerald n. 11S.

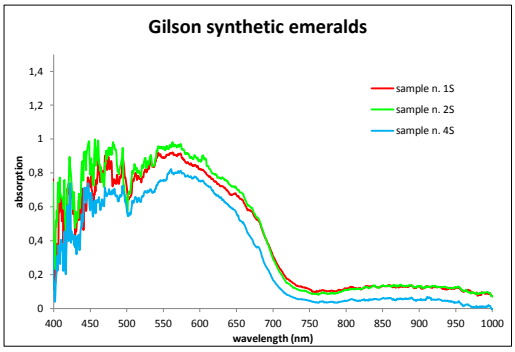

Figure 7. AvaSpec-2048 absorption spectra of Gilson synthetic emerald n. 1S, 2S, 4S.

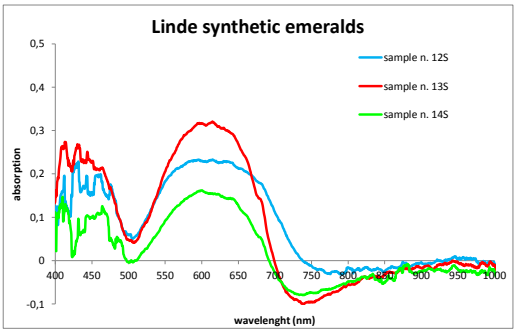

Figure 8. AvaSpec-2048 absorption spectra of Linde synthetic emerald n. 12S, 13S, 14S.

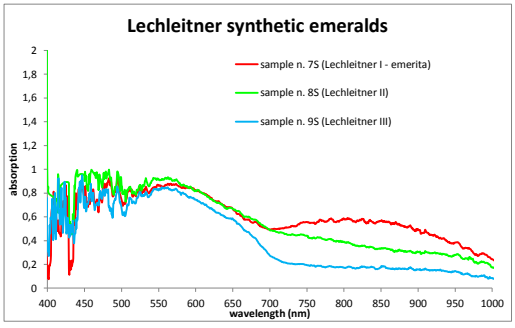

Figure 9. AvaSpec-2048 absorption spectra of Lechleitner synthetic emerald n. 7S, 8S, 9S.

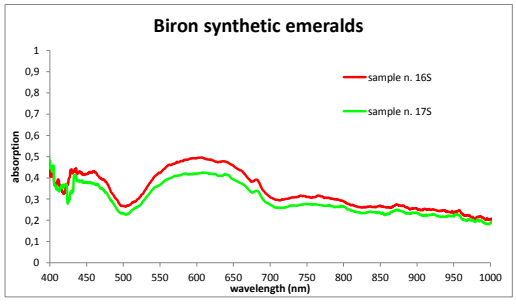

Figure 10. AvaSpec-2048 absorption spectra of Biron synthetic emerald n. 16S, 17S.

presence of iron is not observed.

- Gilson synthetic samples (Figure 7).
  In the spectra of all Gilson synthetic emeralds we observe, at low wavelengths, a high ground noise, that makes difficult to recognize and identify the absorption peaks in a range between 400 to 500 nm. We also observe a broad band centered at about 550 nm that is due to Cr^{3+} (Wood et al., 1968).

Hydrothermal synthesis

- Linde (Figure 8).
  The spectra of Linde emeralds show a negative absorption in the IR region. All the analyzed samples show a broad band at 600 nm and absorption peaks at 415, 430, 480 and 680, related to the presence of Cr^{3+} ions (Wood et al., 1968). We also observe an absorption peak at 465 nm, related to Fe^{3+} (Wood et al., 1968).
- Lechleitner synthetic samples (Figure 9).
  All the Lechleitner samples show a high ground noise at low wavelengths.
  The spectra of the sample Lechleitner I (*emerita*) is very similar to that of natural emeralds; indeed, we observe a broad absorption band centered at 850 nm like the natural samples from Russia. This similarity can be related to the presence of a natural beryl seed within the gemstone. In this sample we also observe some absorption peaks at about 440 and 480 nm, related to Cr^{3+} (Wood et al., 1968).
  In the sample Lechleitner II, the absorption peaks at 440 and 480 nm, related to chromium ions, are also present (Wood et al., 1968).
  The spectrum of the sample Lechleitner III is completely different from the previous ones. The absorption values in the IR range are low, like in the other synthetic emeralds. This sample, however, shows higher ground noise at low wavelengths. Absorption peaks at 420 and 480 nm, due to the presence of Cr^{3+} are also present (Wood et al., 1968).
- Biron synthetic samples (Figure 10).
  The spectra of the Biron synthetic emeralds show a broad band at 600 nm and absorption peaks at 430 and 680 nm, related to Cr^{3+} ions (Wood et al., 1968; Adamo et al., 2005). Another broad band at 450 nm, and absorption peaks at 410 and 460 nm, due to Fe^{3+}, are also present (Wood et al., 1968).

Discussion

This work shows how the new AvaSpec-2048 technique, if supported by the classic gemological analyses, allow to distinguishing natural emeralds from synthetic ones, and also recognize the different typologies of synthesis. The instrument has been tested in the conditions most common in laboratories, that are on gemstones already faceted and not oriented along crystallographic directions.

The use of refractive index and specific gravity to discriminate the natural emeralds from the synthetic should be approached with great prudence as the relative values frequently overlap.

The observation of the gemstones under the microscope allows identification of the typical inclusions and textures of both natural and synthetic samples; this represents a further important support for a correct discrimination between the two typologies.

Spectrometric analyses performed with AvaSpec-2048 proved to be very useful to distinguish the studied samples; this instrumentation can therefore be recommended as a new support for gemological laboratories. The absorption spectra obtained with AvaSpec-2048 are comparable with those reported in literature obtained with other techniques; discrepancies regard only some minor absorption effects and are due to the fact that the samples have not been cut following the

crystallographic orientation.

Several parameters can improve the intensity and resolution of the absorption spectra. The carat of the gemstones, if higher than 0.60 ct allows obtaining better and well-defined absorption spectra. Under this carat the spectra appear very disturbed with a resolution not adequate to recognize absorption bands and peaks. Also the typologies of cut can influence the quality of the spectra: the wider the illuminated surface of the sample by the incident light beam, the better the definition of the spectrum.

The intensity of the color of emeralds can also affect the quality of the absorption spectra: a larger number of chromophore elements, or a larger amount of them, increase the visibility of some bands or absorption lines. Equally important, but only in synthetic samples, is the type of nutrient used to get the synthesis; these can be fundamental for the quality of the absorption spectra. Conversely, the presence of typical inclusions in natural and synthetic emeralds doesn't seem to influence the absorption spectra.

A significant advantage of this technique is that the gemstones, when inserted into the sample holder, are heated slightly by the incident light beam, so avoiding damages to the gems. Others advantages of this methodology are the rapidity of acquisition of the spectra and the possibility to perform the measurements at room temperature on the cut gemstones. The technique also allows identifycation of the chemical chromophore elements with different valence, like chromium and iron.

Probably, the most evident defect of this technique is the high background noise at low wavelengths (between 400 nm and 500 nm), that hides and makes difficult the identification of some absorption bands and peaks. This noise is more frequently observed in the synthetic emeralds than in natural ones.

Additional technical improvements may relate to the components of the instrumentation, in order to reduce the background noise at low wavelengths in the absorption spectra, and thus improving their interpretation. For this reason, a better cooling system of the CCD (e.g. a Peltier cell) and a more powerful light source would be desirable.

AvaSpec-2048 could also allow the identification of the provenance of the natural emeralds, but this would require the analysis of a higher number of samples from specific ores of extraction; this research could be related in particular to the new sites of extraction in China, Nigeria and Tanzania.

In conclusion, our paper develops a new methodology of research potentially very interesting for traceability of precious stones, which is a very current topic also for the increasing sensitivity to a "ethical" trade of the gems.

Acknoledgements

The authors are grateful to Mr. Carlo Cerutti for lending us some emerald samples.

References

Anderson B.W. (1987) - Gemmologia pratica. Pagg. 551, IGI.

Bernini D., Caucia F. and Boiocchi M. (2009) - Application of the Vis-NIR Avaspec-2048 portable automatic spectrometer to distinguish GEM quality materials. *Neues Jahrbuch für Mineralogie Abhandlungen*, 185, 281-288.

Boiocchi M., Caucia F. and Zanetti A. (2004) - Gemological and in-situ chemical analyses of emeralds from Vigezzo Valley (Italy) and other world-wide occurences. *Applied Mineralogy*, Pecchio et al. (eds), 2, 529-532.

Fenoll Hach-Alí P., Gervilla Linares F. and López Galindo A. (2007) - Gemas Conceptos básicos y reconocimiento. Ed. Departamento de Mineralogía y Petrología, Instituto Andaluz de Ciencias de la Tierra, Universidad de Granada - Consejo Superior de Investigaciones Cientificas.

Flamini A., Gastoldi L., Grubessi O. and Viticoli S. (1983) - Contributo della spettroscopia ottica ed EPR alla distinzione tra smeraldi naturali e sintetici. *La Gemmologia*, anno IX, n°1/2.

Flamini A., Grubessi O. and Mottana A. (1984) - Il sistema chimico del berillo e le sue conseguenze sulle

proprietà fisiche. *La Gemmologia*, anno X, n°1/2.
Leone Alberto (2012) - Avaspec-2048: un innovativo metodo spettroscopico per discriminare i minerali qualità gemma - Le pietre verdi. Tesi sperimentale di Laurea in Scienze della Natura. Università di Pavia (A.A. 2010/2011).
Leone A., Caucia F. and Boiocchi M. (2012) - The Avaspec 2048 portable spectrometer as a new spectroscopic method for identification of green gem-quality minerals. III Convegno Nazionale Gemmologia Scientifica, 24-25 settembre.
Leone Angelo (1993) - Giacimenti di smeraldo e relative inclusioni. *Scienza delle Gemme*, anno V, n°2.
Leone E. and Cumo C. (1985) - Gemme naturali e artificiali, Editrice ELLECI.
Wood D.L. and Nassau K. (1968) - The Characterization of Beryl and Emerald by visible and infrared absorption spectroscopy. *American Mineralogist*, 53, 777-800.

Submitted, November 2014 - Accepted, February 2015